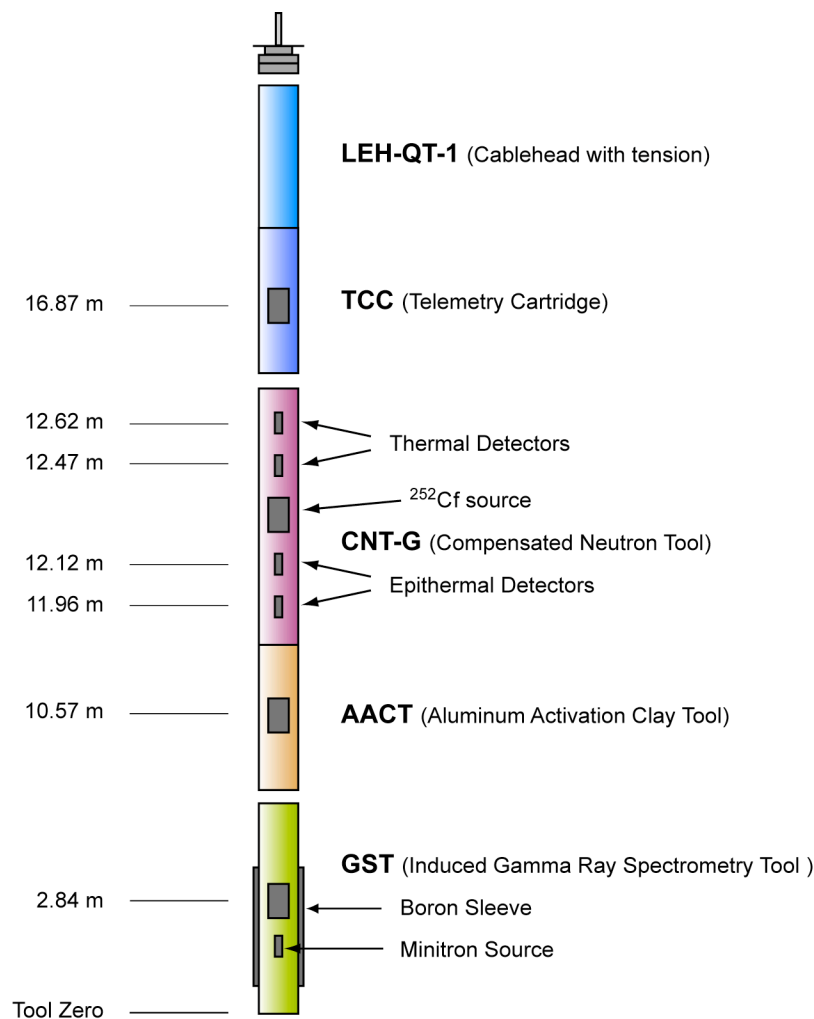


## Leg 157: Geochemical Processing Report

(based on: Bristow, J. et al. (1995). Processing of geochemical data. In Schminke H. U., Weaver, P. P. E., Firth, J. V., et al., Proc. ODP, Init. Reports, 157: College Station, TX (Ocean Drilling Program), 42-44.)

### Geochemical Tool String

The Schlumberger geochemical tool string consists of four logging tools: the natural gamma-ray tool (NGT) the compensated neutron tool (CNT), the aluminum activation clay tool (AACT), and the gamma-ray spectrometry tool (see figure below). The natural gamma-ray tool is located at the top of the tool string, so that it can measure the naturally occurring radio nuclides, Th, U, and K, before the formation is irradiated by the nuclear sources contained in the other tools below. The compensated neutron tool, located below the natural gamma-ray tool, carries a low-energy californium source ( $^{252}\text{Cf}$ ) to activate the Al atoms in the formation. The aluminum activation clay tool below subtracts out the aluminum activation background radiation and a reading of formation Al is obtained (Scott and Smith, 1973).



The gamma-ray spectrometry tool, at the base of the string, carries a pulsed neutron generator to bombard the borehole and formation and an NaI(Tl) scintillation detector, which measures the spectrum of gamma rays generated by neutron-capture reactions. Because each of the elements measured (silicon, iron, calcium, titanium, sulfur, gadolinium, and potassium) is characterized by a unique spectral signature, it is possible to derive the contribution (or yield) of each of them to the measured spectrum and, in turn, to estimate their abundance in the formation. The GST also measures the hydrogen and chlorine in the borehole and formation, but the signal for these elements is almost entirely due to seawater in the borehole, and they are hence of little value.

The only major rock-forming elements not measured by the geochemical tool string are magnesium and sodium; the neutron-capture cross-sections of these elements are too small relative to their typical abundance for the tool string to detect them. A rough estimate of Mg+Na can be made by using the photoelectric factor (PEF) measured by the lithodensity tool. This measured PEF is compared with a calculated PEF (a summation of the PEF from all of the measured elements). The separation between the measured and calculated PEF is, in theory, attributable to any element left over in the formation (i.e., Mg and Na). Further explanation of this technique is found in Hertzog et al. (1989). This calculation was not implemented on the geochemical data from Leg 157 as the (Mg+Na) component was generally below the detection resolution of this technique (Pratson et al., 1993).

## **Data Reduction**

The well log data from the Schlumberger tools have been transmitted digitally up a wireline and recorded on the JOIDES Resolution in the Schlumberger Cyber Service Unit (CSU). The results from the CSU have been processed to correct for the effects of drilling fluids, logging speed, and pipe interference. Processing of the spectrometry data is required to transform the relative elemental yields into oxide weight fractions. The processing is performed with a set of log interpretation programs written by Schlumberger that have been modified to account for the lithologies and hole conditions encountered in ODP holes. The processing steps are summarized below:

### **Step 1: Reconstruction of relative elemental yields from recorded spectral data**

The first processing step uses a weighted least-squares method to compare the measured spectra from the geochemical spectrometry tool with a series of standard spectra in order to determine the relative contribution (or yield) of each element. Whereas six elemental standards (Si, Fe, Ca, S, Cl, and H) are used to produce the shipboard yields, three additional standards (Ti, Gd, and K) can be included in the shore-based processing to improve the fit of the spectral standards to the measured spectra (Grau and Schweitzer, 1989). Although these additional elements often appear in the formation in very low concentrations, they can make a large contribution to the measured spectra, because they have large neutron-capture cross-sections. For example, the capture cross-section of Gd is 49,000 barns, that of Si 0.16 barns (Hertzog et al., 1989). Gd is, therefore, included in the calculation of a best fit between the measured and the standard spectra. The elemental standards (Si, Ca, Fe, Ti, Gd, K, Cl, and H) were used in the spectral analysis step for Holes 950A, 955A and 956B. The spectral standard for S was not used in the final analysis because its concentration was below the detection resolution of the tool in these holes; its

inclusion in the spectral inversion was found to increase the noise level in the other elemental yields. A linear ten point (5 ft, 1.52 m) moving average was applied to the output elemental yields to increase the signal to noise ratios.

The processed yields are loaded in the files

950A-yields.dat

955A-yields.dat

956B-yields.dat.

## Step 2: Depth-shifting

Geochemical processing involves the integration of data from the different tool strings; consequently, it is important that all the data are depth-correlated to one reference logging run. A total gamma-ray curve (from the gamma-ray tool, which is run on each tool string) is usually chosen as a reference curve, based on cable tension (the logging run with the least amount of cable sticking) and cable speed (tools run at faster speeds are less likely to stick). During Leg 157, the depth reference run was taken from the DIT/LSS/NGT and DIT/LSS/HLDT/CNTG/NGT tool string for Holes 950A and 956B, respectively, and from the geochemical tool string for Hole 955A.

## Step 3: Calculation of total radioactivity and Th, U, and K concentrations

The third processing routine calculates the total natural gamma radiation in the formation as well as concentrations of Th, U, and K, using the counts in five spectral windows from the natural gamma-ray tool (Lock and Hoyer, 1971). This resembles shipboard processing, except that corrections for hole-size changes are made in the shore-based processing of these curves. A Kalman filter (Ruckebusch, 1983) is applied to minimize the statistical uncertainties in the logs, which would otherwise create erroneous negative readings and anti-correlation (especially between Th and U). At each depth level calculations and corrections also were performed for K contained in the mud. This K correction is particularly useful where KCl is routinely added to the hole: because of dispersion, however, it is difficult to know exactly how much K is in the borehole. The outputs of this program are: K (wet wt %), U (ppm), and Th (ppm), along with a total gamma-ray curve and a computed gamma-ray curve (total gamma ray minus U contribution).

The processed gamma-ray data are loaded in the files

950A-ngt.dat

955A-ngt.dat

956B-ngt.dat.

The processed data are displayed in the plots

950A.ngt.1.gif

950A.ngt.2.gif

955A.ngt.1.gif

955A.ngt.2.gif

955A.ngt.3.gif

956B.ngt.1.gif

956B.ngt.2.gif.

#### Step 4: Calculation of Al concentration

The fourth processing routine calculates an Al curve using four energy windows, while concurrently correct for natural activity, borehole fluid neutron-capture cross-section, formation neutron-capture cross-section, formation slowing-down length, and borehole size. Porosity and density logs are needed in this routine to convert the wet weight percent K and Al curves to dry weight percent. Porosity logs were calculated from the medium induction logs for all three holes using the relationship of Archie (1942); each had a good correlation with available core porosity measurements. The bulk density logs were used for Holes 950A and 956B, the latter of which was edited to remove extreme low values caused by a rugose borehole. The log density values for Hole 955A showed a very poor correlation in parts with core bulk density measurements (see Site 955), and as a result the interpolated core porosity measurements were used as input in the aluminum calculation.

A correction is also made for Si interference with Al; the  $^{252}\text{Cf}$  source activates the Si, producing the aluminum isotope,  $^{28}\text{Al}$  (Hertzog et al., 1989). The program uses the Si yield from the gamma-ray spectrometry tool to determine the Si background correction. The program outputs dry weight percentages of Al and K, which are used in the calculation and normalization of the remaining elements.

#### Step 5: Normalization of elemental yields from the GST to calculate the elemental weight fractions

This routine combines the dry weight percentages of Al and K with the reconstructed yields to obtain dry weight percentages of the GST elements using the relationship:

$$W_i = F Y_i / S_i$$

where

- $W_i$  = dry weight percentage of the i-th element
- $F$  = normalization factor determined at each depth interval
- $Y_i$  = relative elemental yield for the i-th element
- $S_i$  = relative weight percentage (spectral) sensitivity of the i-th element

The normalization factor,  $F$ , is a calibration factor determined at each depth from a closure argument to account for the number of neutrons captured by a specific concentration of rock elements. Because the sum of oxides in a rock is 100%,  $F$  is given by

$$F (\sum X_i Y_i / S_i) + X_K W_K + X_{Al} W_{Al} = 100$$

where

- $X_i$  = factor for the element to oxide (or carbonate) conversion
- $X_K$  = factor for the conversion of K to  $\text{K}_2\text{O}$  (1.205)
- $X_{Al}$  = factor for the conversion of Al to  $\text{Al}_2\text{O}_3$  (1.889)
- $W_K$  = dry weight percentage of K determined from natural activity

WAl = dry weight percentage of Al determined from the activation measurement

The sensitivity factor,  $S_i$ , is a tool constant measured in the laboratory, which depends on the capture cross-section, gamma-ray production, and detection probabilities of each element measured by the GST (Hertzog et al., 1989).

The factors  $X_i$  are simply element to oxide (or carbonate, sulfate) conversion coefficients and effectively include the O, C or S bound with each element. In processing the GLT data the correct choice of  $X_i$  is important in the closure algorithm described above and requires geological input. In most lithologies the elements measured by the tool occur in silicates where the compositions can be expressed completely as oxides.

With carbonate or carbonate-rich lithologies the measured calcium is more likely to be present as  $\text{CaCO}_3$  ( $X_{\text{Ca}}$ : 2.497) than as the oxide ( $\text{CaO}$ ;  $X_{\text{Ca}}$ : 1.399). A good indication of the choice of calcium conversion factors can often be gained from shipboard X-ray diffraction (XRD) and  $\text{CaCO}_3$  measurements, which estimate acid-liberated  $\text{CaCO}_3$ . In the absence of suitable shipboard data a rough rule of thumb is generally used such that if elemental Ca is below 6% then all Ca is assumed to be in silicate, above 12%, in carbonate. Ca concentrations between these figures are converted using linear interpolation. On Leg 157, the  $\text{CaCO}_3$  factor was used.

Steps 6-7: Calculation of oxide percentages and statistical uncertainty

These routines convert the elemental weight percentages into oxide percentages by multiplying each by its associated oxide factor (Table 1); finally the statistical uncertainty of each element is calculated, using methods described by Grau et al. (1990) and Schweitzer et al. (1988). This error is strongly related to the normalization factor,  $F$ , which is calculated at each depth level. A lower normalization factor represents better counting statistics and therefore higher quality data.

The oxide weight percentages are loaded in the files

950A-oxides.dat

955A-oxides.dat

956B-oxides.dat.

The statistical uncertainties are loaded in the files

950A-oxierr.dat

950A-elerr.dat

955A-oxierr.dat

955A-elerr.dat

956B-oxierr.dat

956B-elerr.dat.

Core data are loaded in the files

950A-core.dat

955A-carb.dat

955A-xrf.dat

956B-core.dat.

Table 1. Oxide/carbonate factors used in normalizing elements to 100% and converting elements to oxides/carbonates.

Element	Oxide/carbonate	Conversion factor
Si	SiO <sub>2</sub>	2.139
Ca	CaCO <sub>3</sub>	2.497
Fe	FeO*	1.358
K	K <sub>2</sub> O	1.205
Ti	TiO <sub>2</sub>	1.668
Al	Al <sub>2</sub> O <sub>3</sub>	1.889

## References

Archie, G. E. (1942). The electrical resistivity log as an aid in determining some reservoir characteristics. Transactions of the American Institute of Mining Engineers, 146: 54-63.

Grau, J. and Schweitzer, J.S. (1989). Elemental concentrations from thermal neutron capture gamma-ray spectra in geological formations. Nuclear Geophysics 3(1): 1-9.

Grau, J. A., Schweitzer J.S. and Hertzog, R.C. (1990). Statistical uncertainties of elemental concentrations extracted from neutron-induced gamma-ray measurements. IEEE Transactions on Nuclear Science, 37(6): 2175-2178.

Hertzog, R., Colson, L., Seeman, B., O'Brien M., Scott, H., McKeon, D., Grau, J., Ellis, D., Schweitzer, J. and Herron, M. (1989). Geochemical logging with spectrometry tools. SPE Formation Evaluation, 4(2): 153-162.

Lock, G. A. and Hoyer, W. A. (1971). Natural gamma-ray spectral logging. The Log Analyst, 12(5): 3-9.

Pratson, E. L., Broglia, C. and Jarrard, R. (1993). Data Report: Geochemical well logs through Cenozoic and Quaternary sediments from Sites 815, 817, 820, 822, and 823. In McKenzie, J. A., Davies, P. J., Palmer-Julson, A. et al., Proc. ODP, Sci. Results, 133: College Station, TX (Ocean Drilling Program), 795-818.

Ruckebusch, G. (1983). A Kalman filtering approach to natural gamma-ray spectroscopy in well logging. IEEE Trans. Autom. Control., AC-28: 372-380.

Schweitzer, J. S., Grau, J.A. and Hertzog, R.C. (1988). Precision and accuracy of short-lived activation measurements for in situ geological analyses. Journal of Trace and Microprobe Techniques, 6(4): 437-451.

Scott, H. D. and Smith, M. P. (1973). The aluminum activation log. The Log Analyst, 14(5): 3-12.

For further information or questions about the processing, please contact:

Cristina Broglia

Phone: 845-365-8343

Fax: 845-365-3182

E-mail: [chris@Ideo.columbia.edu](mailto:chris@Ideo.columbia.edu)

Trevor Williams

Phone: 845-365-8626

Fax: 845-365-3182

E-mail: [trevor@Ideo.columbia.edu](mailto:trevor@Ideo.columbia.edu)